

Infrared imaging of a multi-zone condenser for heat transfer coefficients assessment

Rémi Dickes, Olivier Dumont and Vincent Lemort*

*Thermodynamics Laboratory
Aerospace and Mechanical Engineering Department
University of Liège, Liège, Belgium*

**Corresponding author (rdickes@ulg.ac.be)*

Abstract:

Although crucial for simulations, a proper identification of the convective heat transfer coefficients in multi-zone heat exchangers is a challenging task. While well instrumented thermal systems permit to accurately record the energy balance in such components, the sole knowledge of the global heat transfer rate is not enough to reliably assess these coefficients. In this work, it is proposed to use the zones spatial distribution (i.e. the spatial fraction occupied by the liquid phase, the vapour phase and/or the two-phase regions) as a second identification criteria. An air-cooled condenser into which flows R245fa is considered as case study and a dedicated infrared imaging method is presented to assess the spatial distribution of its different phases. These new data, combined with standard heat transfer rate measurements, are exploited to identify the best heat transfer correlations pre-selected from the scientific literature. In order to further improve the model predictions, the original heat transfer correlations are ultimately adjusted so as to best fit both the global heat transfer rate and the zones distribution data.

Keywords:

Infrared camera, Heat Transfer Coefficients, HVAC, ORC, Heat exchangers, Zones distribution.

1. Introduction

Heat exchangers are crucial components in thermal systems allowing efficient heat transfers between hot and cold media. In rating problems, the objective is commonly to evaluate the amount of energy transferred through a specific component based on its geometry and the fluids supply conditions only. Unlike in steam power plants or higher-capacity systems, small-scale organic Rankine cycles and HVAC systems often employ single heat exchangers to perform the complete heating and cooling of their working fluid. While being easier to put in practice,

such a simple configuration complicates some modelling aspects. Since the fluid experiences a phase-change in both evaporators and condensers, several states of fluid (i.e. liquid, two-phase and/or vapour phases) often coexist in a same component. In order to account for this spatial division, a common approach is to simulate the heat exchanger with a one-dimensional moving-boundary method [1]. Each zone i is considered individually and simulated with classic heat transfer equations, i.e.

$$A_i = \frac{\dot{Q}_i}{U_i F_i \Delta T_{log,i}} \quad (1)$$

where

$$\frac{1}{A_i U_i} = \frac{1}{H_{h,i} A_{h,i} \eta_{s,h,i}} + \frac{t_i}{k_i A_i} + \frac{1}{H_{c,i} A_{c,i} \eta_{s,c,i}} \quad (2)$$

and

- A_i is the surface area occupied by the i^{th} zone;
- U_i is the global heat transfer coefficient;
- $\Delta T_{log,i}$ is the zone logarithm mean temperature difference (LMTD) between the two fluids;
- F_i is the LMTD correction factor to apply if the heat exchanger is not of counterflow;
- t_i and k_i are the wall thickness and conductivity;
- $\eta_{s,h,i}$ and $\eta_{s,c,i}$ are the surface efficiency on each side (< 1 in case of finned geometry, $= 1$ otherwise);
- $H_{h,i}$ and $H_{c,i}$ are the convective heat transfer coefficients (CHTCs) on each side;

The effective heat transfer between the two fluids is thus calculated such as the total surface area occupied by the different zones corresponds to the actual geometry of the component, i.e.

$$A_{HEX} = \sum_{i=1}^N A_i \quad (3)$$

As highlighted in Equation (2), a proper modelling of the heat exchangers is highly affected by the ability to characterize the convective heat transfer coefficients (CHTCs) in the different zones. Although crucial, the identification of these coefficients from experimental measurements is quite challenging. Most test rigs only feature thermo-hydraulic sensors at the inlet and outlet ports of the heat exchangers which permit “solely” to calculate the global heat transfer rate within the component (i.e. $\dot{Q} = \dot{m}(h_{su} - h_{ex})$). However, such a knowledge of the global heat transfer is not enough to properly identify these coefficients. Indeed, since several convective heat transfer coefficients intervene in the computation of the thermal performance, and because multiple zones coexist in a same component, very different sets of coefficients can

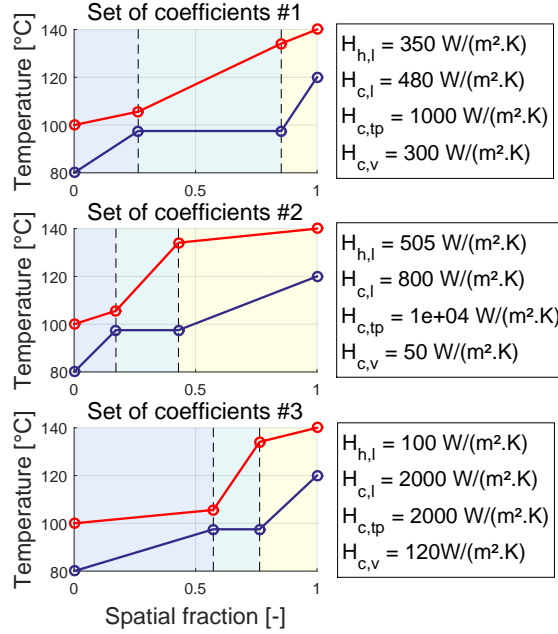


Figure 1: Identical heat transfer in an evaporator with three different sets of convective heat transfer coefficients (temperature profile vs. normalized length).

lead to the exact same heat transfer predictions. Such a situation is illustrated in Figure 1 with an evaporator. As evidenced with three different scenarios, the same heat transfer rate (i.e. the outlet temperatures are identical) is retrieved with significantly different combinations of CHTCs. Therefore, unless the experimental data features single-zone conditions (i.e. operating conditions with only a liquid-phase, a vapour-phase or a two-phase flow in the HEXs), the identification of the CHTCs based only on heat transfer rate measurements will more likely lead to wrong results since there is an infinity of solutions. Alternatively, one may use heat transfer correlations found in the literature to estimate the coefficients $H_{h,i}$ and $H_{c,i}$. However, these correlations are generally purely empirical and calibrated to fit experimental data gathered on specific test rigs. Their extrapolability to other fluids, geometries or operating conditions is often controversial and multiple candidates can be considered to simulate a same situation. While these correlations provide good guesses to estimate the CHTCs, they generally need some adjustments to better fit another case study, which leads to the same identification issue as mentioned above. An interesting solution to this problem appears by looking back to Figure 1. As evidenced with the temperature profiles, the heat transfer coefficients do not only play a role on the thermal performance, they also impact the spatial distribution of the different zones. This observation is extremely important and has one crucial outcome: any knowledge about the zones distribution in a heat exchanger can help *to identify* the convective heat transfer coefficients. This work aims to illustrate how an infrared camera can be exploited to this end.

The paper is organized as follows. The heat exchanger considered as case study is first presented in Section 2. Then Section 3 describes the infrared imaging method developed to record the

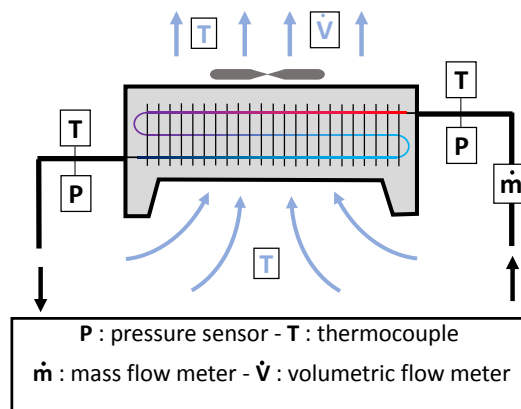
zones distribution. This method, combined with standard global heat transfer measurements, are ultimately exploited to identify the convective heat transfer coefficients in Section 4.

2. Case study description

In order to illustrate this work, an air-cooled condenser integrated in a 2 kW_e ORC system is taken as case study. Depicted in Figure 2a, it is a fin coil heat exchanger developed by Alfa Laval (model Solar Junior 121) made of 13 parallel channels, each effectuating 12 passes in a matrix of plain fins. Condensing R245fa is pumped across the tubes while ambient air is pulsed with a variable-speed fan placed at the top of the condenser. As shown in Figure 2b, the test rig is fully monitored with thermocouples, flow meters and pressure sensors so the condenser heat transfer rate can be evaluated accurately. An extensive experimental campaign was conducted with the ORC system which led to a complete database including more than 300 steady-state points ¹. The condenser heat transfer performance (i.e. \dot{Q}_{cd}) is thus fully characterized over a wide range of conditions. As mentioned in the introduction, however, these global heat transfer data are not enough to reliably identify the convective heat transfer coefficients. In parallel to these thermo-hydraulic measurements, the following IR imaging method was applied.



(a) Photo of the system.



(b) Scheme of the condenser.

Figure 2: Fin coil condenser of an ORC system taken as case study.

3. Infrared imaging method

In order to perfectly assess the zones distribution, the ideal solution would be to continuously record the fluid temperature all along its path in the condenser. In practice, the tubes into

¹The work presented in this paper is part of more general investigation focusing on the charge distribution in ORC systems. The experimental campaign did not aim to characterize the condenser only, but also all the other components and the ORC charge inventory. For any further detail regarding the ORC unit, the experimental campaign or the results, please refer to the author's PhD thesis [2].

which flows the working fluid are placed in a matrix of plain fins and most of them are invisible from the outside. However, by removing the side plates of the condenser, one can visualize the end-tips of these tubes. If the end-tips are observed with an infrared camera as shown in Figure 3, the temperature evolution along the channels can be reconstructed. Although the temperature profile is not continuously monitored (i.e. the temperature is rated at 13 discrete points), these infrared (IR) data help to more precisely localize the frontiers between the liquid, the vapour and the two-phase zones.

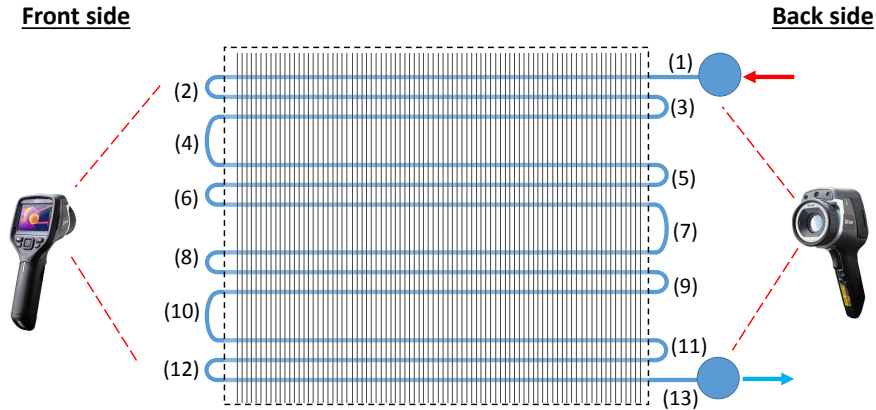


Figure 3: Configuration and position numbering for one channel in the condenser.

For every operational point tested with the ORC system, a set of 4 infrared (IR) photos is captured with a *FLIR E50* camera. Each photo is shot from a specific point of view (two at the front, two at the back) in order to fully monitor the condenser temperature profile. For instance, the photos collected for one operating point are given in Figure 4. The IR photos #1 and #4 offer an overview of the temperature distribution in the complete tubes bank, while photos #2 and #3 focus on a specific channel. After verifying that the temperature distribution along the heat exchanger is quasi-homogeneous (i.e. that there is no significant discrepancies between the different channels), the temperature profile along one typical path is extracted. To this end, a semi-automated algorithm is run to quickly locate the end-tips of this particular channel on the different photos (i.e. the red crosses in Figure 4). The temperatures are then retrieved from the IR data corresponding to the selected pixels. In order to avoid any viewing angle effect [3], the pixels locations are selected so the tube outer surface is always normal to the IR camera. A post-treatment algorithm is then applied to merge the temperature profiles identified on the front side (i.e. from photo #2) and the back side (i.e. from photos #3 and #4) of the condenser. Because the tube emissivity is not perfectly known and because the photos are not taken from the same distance, the two temperature profiles cannot be simply superposed. Indeed, each photo gives an image of the relative temperature gradient seen from a specific point of view, but they do not share the same absolute reference. To overcome this issue, the temperatures profiles are shifted and combined so as to comply with the saturation temperatures gathered by the pressure sensors. More specifically, the merging algorithm relies in two main steps, i.e.

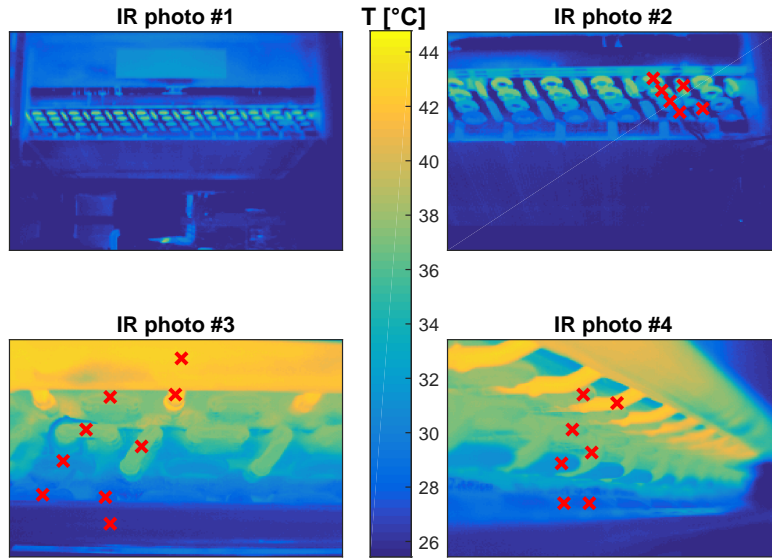


Figure 4: Example of IR photos taken for one operational point (the red crosses correspond to the locations where the temperatures are evaluated).

1. to identify the pseudo-isothermal region in which occurs the condensation process on both front and back sides;
2. to merge the front and the back temperature profiles assuming a continuity in the two-phase region.

For instance, the temperature profile identified for the previous example is depicted in Figure 5. As discussed in the next section, such a result offers very valuable information to better identify the convective heat transfer coefficients. However, the proposed infrared imaging method has two important limitations that must be pointed out:

- Because the temperature profile is not continuously recorded but evaluated at 13 discrete points, the zones distribution is known with a limited accuracy. In the example given in Figure 5, the boundary between the two-phase and the vapour zones is not perfectly assessed. Indeed, it can be located at any place between positions #1 and #2. Similarly, the frontier between the liquid and the two-phase regions is located anywhere between positions #7 and #8. Combining these two uncertainties, the spatial fraction occupied by the two-phase region is known with an absolute accuracy of $\pm 16.7\%$. The spatial fraction of the single-phase zones, however, is estimated within an error of $\pm 8.3\%$.
- The IR photos record the external wall temperature of the tubes which can significantly differ from the bulk conditions of the fluid. The difference between these two values not only depends on the ambient conditions, but also on the convective heat transfer coefficients of the fluid. In two-phase regions, the external wall temperature is close to the internal conditions because the condensing heat transfer coefficient is very high. In single-phase regions, however, the heat transfer coefficient is much lower and a larger

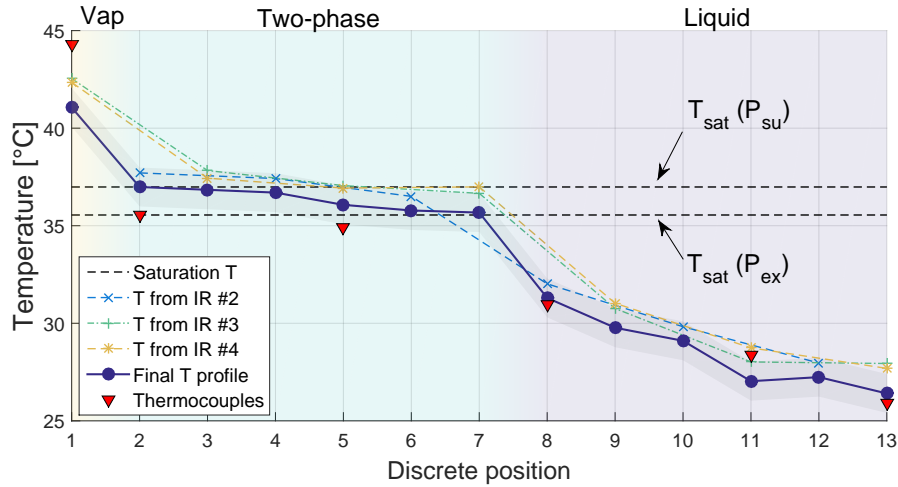


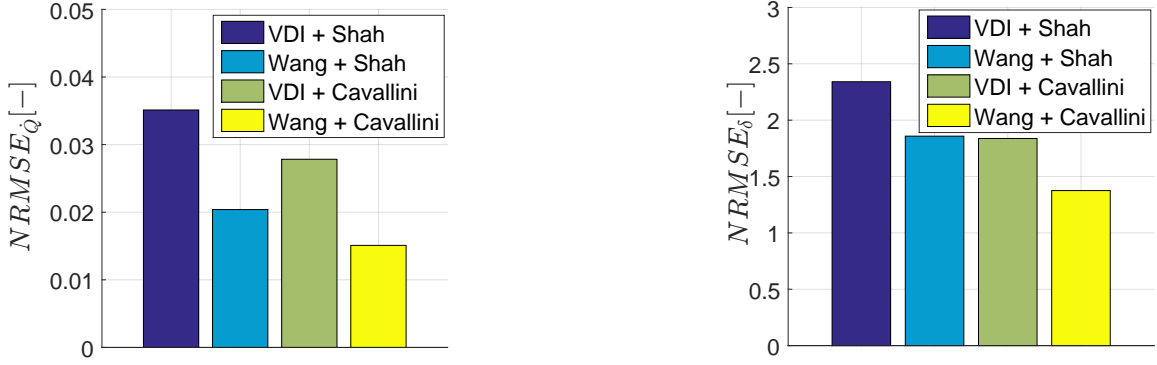
Figure 5: Temperature profiles identify for the example case in Figure 4.

temperature gradient appears between the external wall and the bulk. Such a situation is observable in Figure 5 at the condenser inlet. Because of these radial gradients, the temperature profiles identified with the IR data should only be used for qualitative and not quantitative purposes. The IR observations help to identify the zones boundaries but should not be considered as an exact measurement of the working fluid temperature profile.

Keeping these limitations in mind, this IR imaging method is applied for every point of the experimental campaign conducted with the ORC system. Ultimately, a complete database of temperature profiles and global heat transfer performance is gathered to characterize the condenser operation. As discussed in the next section, these data provide valuable information to identify the various convective heat transfer coefficients.

4. Identification of the convective heat transfer coefficients

The convective heat transfer coefficients can either be fully re-identified from the experimental data but best practice is to exploit state-of-the-art correlation as initial guesses. For the present case study, the coefficients of three flow regimes must be assessed, namely for single-phase and condensing conditions of the working fluid, so as for the air flow across the plain fins and the tubes bank. Single-phase flows inside smooth horizontal tubes constitutes probably the best known situation in the literature. In this work, a single correlation is considered given the large credit recognized for its heat transfer predictions and its wide range of validity. This model is the one of Gnielinski [4]. For each of the other flow regimes (i.e. the condensation of the working fluid and the air flow), two candidates are selected from well-quoted correlations in the literature, namely the models of Shah [5] and of Cavallini et al. [6] for the condensation, and the models of Wang et al. [7] and of the VDI [4] for the air flow. Ultimately, four different models of the condenser are considered (i.e. every combination between the two condensing models and the two air-flow correlations) and compared to the experimental data. To assess



(a) Fitting of the global heat transfer rate.

(b) Fitting of the zones spatial distribution.

Figure 6: Comparison of the four set of correlations to simulate the condenser.

the validity of the different models, their predictions are discussed both in terms of global heat transfer rate **and** zones spatial distribution. In order to quantify the compliance between the simulation results with the experimental data, normalized root mean square errors (NRMSEs) are computed for each criteria, i.e. one for the global heat transfer predictions

$$NRMSE_{\dot{Q}} = \sqrt{\sum_{i=1}^N \left(\frac{\dot{Q}_{sim,i} - \dot{Q}_{exp,i}}{\dot{Q}_{exp,max} - \dot{Q}_{exp,min}} \right)^2} \quad (4)$$

and one for the zones spatial distribution i.e.

$$NRMSE_{\delta} = \sqrt{\sum_{i=1}^N \left(\frac{|\delta A_{v,i}|^2 + |\delta A_{l,i}|^2 + |\delta A_{tp,i}|^2}{3} \right)^2} \quad (5)$$

where

$$\delta A_{v,i} = \frac{A_{v,sim,i} - A_{v,IR,i}}{A_{cd,tot}} \quad (6)$$

$$\delta A_{l,i} = \frac{A_{l,sim,i} - A_{l,IR,i}}{A_{cd,tot}} \quad (7)$$

$$\delta A_{tp,i} = \frac{A_{tp,sim,i} - A_{tp,IR,i}}{A_{cd,tot}} \quad (8)$$

and $A_{cd,tot}$ is the total surface area of the condenser and $A_{j,sim,i}/A_{j,IR,i}$ are the areas predicted and experimentally monitored for the different zones for the i^{th} point. The results gathered for the four models are depicted in Figure 6. For the sake of convenience, these models are referred to as model *A*, *B*, *C* and *D* in the following discussion. Comparing the different NRMSE factors, the model demonstrating the poorest fit is the model *A*. In comparisons to the three others, this model leads to the largest residuals for both the global heat transfer and spatial

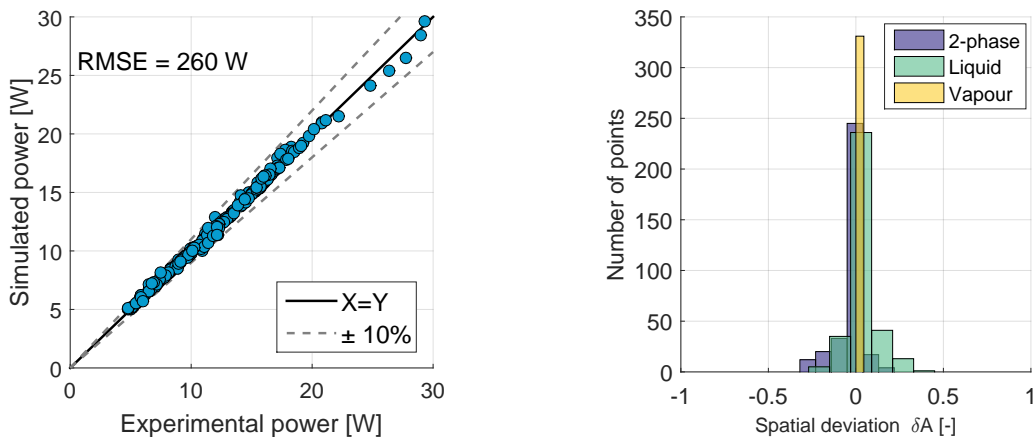
zone distributions. The models B and C show antagonist benefits. While the first one much better replicates the condenser heat transfer rate, the model C has a better compliance with the zones spatial distribution. The best candidate among the four options investigated appears to be the model D , i.e. the one coupling the correlations of Wang et al. [7], of Cavallini et al. [6] and of Gnielinski [4]. A good starting point is thus to consider these correlations to calculate the convective heat transfer coefficients. In order to further improve the model predictions, these CHTC correlations can be adjusted so as to better comply with the experimental data. To this end, each correlation is simply scaled by a constant factor c_j as proposed in [8], i.e.

$$Nu_j^* = c_j Nu_j \quad (9)$$

where Nu_j is the original Nusselt number predicted by the correlation. To ensure the most reliable model, the calibration of the c_j factors is conducted by minimizing the residuals committed on both the heat transfer rate and the zones repartition predictions, i.e.

$$\min_{c_j} F = \Psi \underbrace{\sqrt{\sum_{i=1}^N \left(\frac{\dot{Q}_{sim,i} - \dot{Q}_{exp,i}}{\dot{Q}_{exp,max} - \dot{Q}_{exp,min}} \right)^2}}_{NRMSE_{\dot{Q}}} + \Omega \underbrace{\sqrt{\sum_{i=1}^N \left(\frac{|\delta A_{v,i}|^2 + |\delta A_{l,i}|^2 + |\delta A_{tp,i}|^2}{3} \right)^2}}_{NRMSE_{\delta}} \quad (10)$$

where Ω and Ψ are two scaling values giving the same weight at both criteria. The correction factors identified by this optimization are specified in Table 1 and the results gathered with the adjusted correlations are depicted in Figure 7. As demonstrated, a good agreement is now observed for both heat transfer and spatial distribution predictions.



(a) Experimental vs. simulated heat transfers

(b) Histogram on spatial distribution errors

Figure 7: Predictions after tuning of the best predictive model.

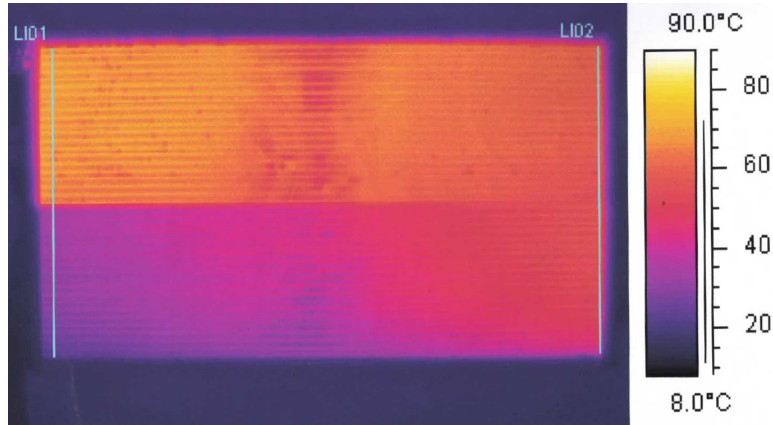


Figure 8: Compact condenser for an automotive application.

5. Conclusion

Although crucial for simulations, a proper identification of the convective heat transfer coefficients in multi-zone heat exchangers is a challenging task. While well instrumented systems permit to accurately record the energy balance in such components, the sole knowledge of the global heat transfer rate is not enough to reliably assess these coefficients. In this work, it is proposed to use the zones spatial distribution (i.e. the spatial fraction occupied by the liquid phase, the vapour phase and/or the two-phase regions) as a second identification criteria. An air-cooled condenser placed in a 2kWe ORC unit is considered as case study and a dedicated IR imaging method is presented to assess the spatial distribution of the different zones. These new data, combined with standard heat transfer rate measurements, are exploited to identify the best heat transfer correlations pre-selected from the scientific literature. Ultimately, it is shown that for the present case study, the correlations of Wang et al. [7], Gnielinski [4] and Cavillini et al. [6] best replicate the experimental observations. In order further improve the model predictions, the original heat transfer correlations are tuned so as to better fit both data on the global heat transfer rate and zones repartition.

The methodology proposed here above is not restricted to the present case study and can be re-applied to many other heat exchanger (HEX) technologies. As long as the temperature evolution can be recorded with an IR camera (as shown in Figure 8 for another example), the zones spatial distribution can be reconstructed and exploited effectively. This method is particularly suited for heat exchangers implying two-phase conditions inside tubes (e.g. finned-tube HEXs, tube-in-tube HEXs, helocoidal HEX, etc.) but could also be extended to other common technologies, like plate heat exchangers (e.g. as demonstrated in [9]).

Appendix

The coefficients identified by minimizing (10) are reported in Table 1. Constitutive equations of the heat transfer correlations are accessible in the corresponding references.

Table 1: Adjusting coefficients of the heat transfer correlations

Zone	Heat transfer correlation	Tuning coefficient
Air-side flow	Wang et al. [7]	$c = 0.8719$
Liquid flow	Gnielinski [4]	$c = 0.7868$
Condensing flow	Cavallini et al. [6]	$c = 1.6$
Vapour flow	Gnielinski [4]	$c = 2.45$

Nomenclature

CHTC	Convective Heat Transfer Coefficient	\dot{Q}	Heat power [W]
HEX	Heat Exchanger	t	thickness [m]
HVAC	Heating Ventilation Air Conditioning	U	Heat transfer coefficient [$W/m^2.K$]
LMTD	Logarithmic Mean Temp. Difference	T	temperature [K]
NRMSE	Normalize Root Mean Square Error		
ORC	Organic Rankine Cycle	c	cold
		cd	condenser
A	surface [m^2]	ex	exhaust
c	coefficient [–]	exp	experimental
ΔT	Temperature difference [K]	h	hot
η	Fin efficient [–]	l	liquid
F	LMTD factor [–]	log	logarithmic
H	Convective Heat Transfer Coeff. [$W/m^2.K$]	sat	saturation
k	Conductivity [W/K]	sim	simulated
\dot{m}	mass flow [kg/s]	su	supply
Nu	Nusselt number [–]	tp	two-phase
P	Pressure [Pa]	v	vapour

References

- [1] Ian H. Bell et al. “A generalized moving-boundary algorithm to predict the heat transfer rate of counterflow heat exchangers for any phase configuration”. In: *Applied Thermal Engineering* 79 (2015), pp. 192–201. URL: <http://linkinghub.elsevier.com/retrieve/pii/S1359431114011570>.
- [2] Rémi Dicks. “Charge-sensitive methods for the off-design performance characterization of organic Rankine cycle (ORC) power systems”. PhD thesis. University of Liège, 2019.

- [3] Giovanni Maria Carlomagno and Gennaro Cardone. “Infrared thermography for convective heat transfer measurements”. In: *Experiments in Fluids* 49.6 (2010), pp. 1187–1218. ISSN: 07234864. DOI: 10.1007/s00348-010-0912-2.
- [4] *VDI Heat Atlas*. 2nd Editio. Springer-Verlag Berlin Heidelberg. ISBN: 9783540778769.
- [5] M. M. Shah. “A general correlation for heat transfer during film condensation inside pipes”. In: *International Journal of Heat and Mass Transfer* 22.4 (1979), pp. 547–556. ISSN: 00179310. DOI: 10.1016/0017-9310(79)90058-9.
- [6] Alberto Cavallini et al. “Condensation in Horizontal Smooth Tubes: A New Heat Transfer Model for Heat Exchanger Design”. In: *Heat Transfer Engineering* 27.8 (2006), pp. 31–38. ISSN: 0145-7632. DOI: 10.1080/01457630600793970. URL: <http://www.tandfonline.com/doi/abs/10.1080/01457630600793970>.
- [7] Chi-chuan Wang, Kuan-yu Chi, and Chun-jung Chang. “Heat transfer and friction characteristics of plain fin-and- tube heat exchangers , part II : Correlation”. In: *International Journal of Heat and Mass Transfer* 43 (2000), pp. 2693–2700.
- [8] Rémi Dickes et al. “Charge-sensitive modelling of organic Rankine cycle power systems for off-design performance simulation”. In: *Applied Energy* 212.January (2018), pp. 1262–1281. ISSN: 0306-2619. DOI: 10.1016/j.apenergy.2018.01.004. URL: <https://doi.org/10.1016/j.apenergy.2018.01.004>.
- [9] Giovanni A. Longo et al. “HFC32 vaporisation inside a Braze Plate Heat Exchanger (BPHE): Experimental measurements and IR thermography analysis”. In: *International Journal of Refrigeration* 57 (2015), pp. 77–86. ISSN: 01407007. DOI: 10.1016/j.ijrefrig.2015.04.017. URL: <http://dx.doi.org/10.1016/j.ijrefrig.2015.04.017>.